C. Bisagni, M.S. Pigazzini
Modelling Strategies for Numerical Simulation of Aircraft Ditching
International Journal of Crashworthiness, Vol. 23, N. 4, 2018, p. 377-394
doi:10.1080/13588265.2017.1328957

INTERNATIONAL JOURNAL OF CRASHWORTHINESS
2018, VOL. 23, NO. 4, 377–394
https://doi.org/10.1080/13588265.2017.1328957

Taylor & Francis
Taylor & Francis Group

Modelling strategies for numerical simulation of aircraft ditching

C. Bisagni[a] and M.S. Pigazzini[b]

[a]Delft University of Technology, Faculty of Aerospace Engineering, Delft, Netherlands; [b]University of California San Diego, Department of Structural Engineering, La Jolla, CA, USA

ABSTRACT

Ditching, which is a controlled landing of an airplane on water, is an emergency condition to be investigated in order to improve the aircraft global crashworthiness. The complex hydrodynamic phenomena involved in ditching events are difficult to simulate and the accuracy of the results depends on the capability to reproduce the forces related to the interaction of the fuselage with the water surface. In the first part of the paper, the vertical impact on water of a rigid sphere is analysed using the explicit solver LS-DYNA in order to compare different modelling strategies. Four models of the fluid domain are presented: Lagrangian, arbitrary Lagrangian–Eulerian, smoothed particle hydrodynamics and hybrid Lagrangian-smoothed particle hydrodynamics. In the second part, the ditching of a scaled simplified airplane is simulated considering two different models for the water region. Experimental data from the literature are used to validate the simulations. The analysis, where the water and the air are modelled with the arbitrary Lagrangian–Eulerian method, shows a better correlation with the experimental data because this formulation can reproduce the suction force which acts on the fuselage and affects significantly the ditching dynamics.

ARTICLE HISTORY
Received 29 December 2016
Accepted 6 May 2017

KEYWORDS
Ditching; fluid-structure interaction; water impact; ALE; hybrid Lagrangian-SPH

Introduction

Ditching is an emergency manoeuvre that consists in a landing on water of an aircraft which is not specifically designed for water landings. An emergency water landing is properly classified as a ditching if all the following conditions subsist [16]: the pilot has either a complete or a partial control of the airplane, the maximum descending rate is 1.5 m/s and the loading conditions do no exceed the design parameters. Although ditching events are considered rare events from a statistical point of view [22], the world-famous accident that occurred in the water of the Hudson River in 2009 [21] focused the attention on the safety issue in case of emergency landings on water.

The dynamics of a ditching manoeuvre is traditionally investigated by means of expensive experimental tests performed on scaled size models. An experimental test might also be required for certification purposes in order to prove that an aircraft complies with the ditching regulations, i.e. CS 25.801, which aims to minimise the possibility of injuries for the passengers in case of accidental landing on water.

Relevant experimental studies on scaled models were performed in the 1950s [8,19,25,28] in order to investigate the influence of the sensitivity of the hydrodynamic forces with respect to different aircraft configuration and under different ditching conditions. However, besides the inherent costs of experimental campaigns, the results obtained from scaled models are affected by inaccuracies related to the scaling of the hydrodynamics phenomena. In the past years, it became clear that the use of numerical simulations, which aim to support the design and the verification process, is also crucial in order to reduce the costs of experimental tests [24].

Since the introduction of fluid-structure interaction (FSI) techniques in commercial finite element (FE) codes, several authors [15,23,30,31] proposed numerical models aiming to investigate the problem of vertical impacts on water of aeronautical structures. While vertical impacts have been extensively analysed both numerically and experimentally [1,2,14,24], there are still difficulties related to the numerical simulation of ditching events [6,11,13,27,29]. This is essentially related to two main factors. First, the validation of numerical models for ditching simulations is problematic because of the substantial lack of experimental data to be used for the correlation. Second, the simulation of the complex physics phenomena, which arise from the interaction of the fuselage with the water surface, is a challenging task from a numerical standpoint.

Therefore, the development of reliable numerical models for the prediction of the hydrodynamic loads is

CONTACT C. Bisagni c.bisagni@tudelft.nl

considered a priority in order to improve the airplanes overall crashworthy design.

This paper focuses on different modelling approaches for FSI problems, with emphasis on the numerical analysis of ditching events. The simulations are performed on a simplified aeronautical fuselage by using the commercial code LS-DYNA. The results obtained using different formulations for the water domain are compared and correlated with the data from an experimental test [19]. The analysis of the distribution of the hydrodynamic pressure, acting on the fuselage, allows for a better understanding of the physics underlying ditching events.

The work is structured as follows: a survey of the formulations available in LS-DYNA for FSI simulations is presented in the first section. Different modelling strategies are then applied for the analysis of a vertical impact on water of a rigid sphere in order to assess the accuracy of the formulations presented in the first section. Then, the work focuses on the simulation of a ditching scenario. Two different modelling strategies are adopted for the fluid region and the results are compared with experimental data taken from literature in order to validate the model. The paper concludes with the analysis of the results: the accuracy of the numerical formulations for ditching applications is investigated and the advantages of each modelling approach are discussed.

Numerical formulations for fluid-structure interaction and ditching

The choice of an appropriate formulation for the discretisation of the fluid domain is critical in the framework of FSI simulations. Several authors [2,5,15,23] adopted Lagrangian FE discretisation in order to simulate vertical impacts on water of both rigid and deformable structures. They found that the Lagrangian approach for the representation of the fluid domain allows to accurately predict the deceleration peak at the initial stage of the impact. However, since in a Lagrangian approach the mesh moves with the material points, this formulation is not suitable to model problems where fluids are subjected to large deformations. Indeed, FE meshes based on a Lagrangian formulation suffer from numerical instabilities and time-step reduction caused by the distortion of the elements.

Conversely, in the Eulerian approach the computational grid is fixed in space and the material flows through the elements. While this formulation allows to handle any arbitrary motion of the fluid domain, it introduces the complexity related to the advection of the material through the mesh. The Eulerian FE approach is typically adopted for fluid mechanics simulations, while its application for the structural analysis poses several challenges because it is inherently difficult to resolve the boundaries of solid geometries.

Hybrid approaches are therefore considered an optimal solution for FSI simulations: a Lagrangian FE mesh is used to discretise the structural components, while the fluid domain is modelled either through an Eulerian or a hybrid formulation. In particular, the arbitrary Lagrangian–Eulerian (ALE) method [4,17,26] is adopted in this paper for the discretisation of the fluid domain. The ALE technique consists in a Lagrangian step followed by a rezoning step, which is performed in order to alleviate the distortion of the mesh. During the rezoning process, the material is transported, or advected, through the elements, while the computational grid is either translated in space or reshaped into its original configuration. In the latter case, the ALE method coincides with the Eulerian formulation. Since the advection process is expensive in terms of computational time, it is preferable to perform an advection step only after a few Lagrangian steps [12] in order to increase the computational performances. The optimal number of Lagrangian steps to be performed before applying the rezoning process depends on the specific problem and, in general, it is required to find a trade-off between the computational time and the accuracy of the analysis.

The use of a mesh-free formulation is an additional alternative to the traditional FE methods for representing fluid domains in FSI applications. The smoothed particle hydrodynamics (SPH) method [20,32] is a particular mesh-free formulation available in LS-DYNA. It is based on the application of an interpolation scheme, which makes use of smoothing kernel functions with a compact support, in order to obtain the governing equations of a discrete system of elements. The particle nature of the SPH formulation makes it suitable for simulations that involve arbitrary large displacements of the material. Therefore, it can be adopted for modelling the fluid domain in FSI simulations, while traditional Lagrangian FEs are used to represents the structural part of the model. The accuracy of the SPH formulation is related to the distribution of the discrete particles relative to each other: in the optimal case a uniform discretisation, where each SPH element is surrounded by the same number of particles, is preferable and particular attention is required to apply local refinement. However, a fine discretisation is required in the region of the FSI in order to capture the small scale hydrodynamics phenomena, while a coarser distribution of the particles would be preferable elsewhere in order to reduce the computational time.

A hybrid Lagrangian-SPH approach has been proposed [6,9,10,29] in order to improve the computational

performances of the pure mesh-free method for the representation of the fluid domain. The proposed solution consists in replacing the discrete SPH particles with Lagrangian solid elements in a limited portion of the domain, wherever the deformations of the fluid region are expected to be small. The interaction of the Lagrangian mesh and the SPH particles is enforced through a penalty contact algorithm. This hybrid approach introduces two major difficulties in the modelling process. The first is the definition of proper contact parameters at the interface between the discrete particles and the FEs. Another problem is represented by the choice of the amount of fluid volume where the SPH particles have to be replaced with Lagrangian elements. The optimal trade-off is to replace as much SPH particles as possible in order to reduce the computational time without affecting the accuracy of the solution.

In the next section, a simple FSI vertical impact problem is analysed and discussed in order to assess the accuracy and the computational performances of the different modelling strategies for the fluid domain.

Vertical drop of a rigid sphere into water

A first series of numerical analyses were performed to simulate the vertical entry of a rigid sphere into calm water. The simulations are based on an experimental reference test case [3,29]. While vertical impacts on water have been already investigated theoretically and experimentally [7,33], the purpose of these simulations is to compare the different modelling strategies for the water domain in terms of accuracy and of computational performances.

Model description

The sphere has a radius of 109 mm and a mass of 3.76 kg. Since the average density is 0.693 g/cm^3, it has a positive buoyancy in water. A rigid-type material is used to model the sphere that is discretised through 3750 Lagrangian quad-node shell elements with an average edge length of 5.75 mm in the impact area. In order to properly detect interpenetrations, the mesh of the sphere should be as refined as the mesh of the water. A Young modulus of 200 GPa is assigned to the rigid-type material in order to compute the contact force that allows the interaction with water. The initial vertical velocity is 11,800 mm/s and the initial gap between the water and the sphere is 30 mm. The gravity is included in the model as an inertial acceleration. The same sphere model is used for all the simulations.

Modelling strategies for water

The water model is based on a linear polynomial equation of state (EOS) that relates the internal pressure to the ratio of the current and the initial density of water, ρ and ρ_0, respectively [12],

$$P = C_0 + C_1\mu + C_2\mu^2 + C_3\mu^3 + (C_4 + C_5\mu + C_6\mu^2)E$$

$$\mu = \frac{\rho}{\rho_0} - 1,$$

where P is the internal pressure and E is the internal energy; μ is set equal to 0 at the initial time. Since the system is assumed to be in equilibrium at the beginning of the simulation, the initial pressure of water is set to zero by $C_0 = 0$. Furthermore, the internal pressure is assumed to be independent from the internal energy; therefore $C_4 = C_5 = C_6 = 0$. The coefficients $C_1 = 2723$ MPa, $C_2 = 7727$ MPa and $C_3 = 14{,}660$ MPa derive from experimental data [29]. All the EOS coefficients used for the vertical impact simulations are listed in Table 1.

A null-type material is used for the fluid because water does not possess any shear stiffness. This material model disregards the deviatoric part of the stress tensor and improves the computational efficiency. The viscous stress is obtained by multiplying the deviatoric strain rate by the kinematic viscosity, which is defined equal to 10^{-3} Pa*s.

A penalty-type contact, which ensures the conservation of the total momentum, is used to enforce the interaction between the water and the sphere. The contact damping is set to zero in order to prevent numerical losses of energy. In addition, since the contact between the water and the sphere is assumed to be frictionless, the static and dynamic Coulomb's friction coefficients are set to zero. This assumption is justified because the mass forces are dominant compared to viscous forces during high speed vertical impacts.

The cavitation is modelled by introducing a cut-off threshold to prevent the pressure from assuming non-physical negative values. This simplified algorithm deletes the elements as soon as their internal pressure falls below a user-specified value. It allows to take into account for the separation of the water spray but it

Table 1. Linear polynomial EOS coefficients for vertical impact simulations.

Material	C_0 (MPa)	C_1 (MPa)	C_2 (MPa)	C_3 (MPa)	C_4	C_5	C_6
Water	0	2723	7727	14,660	0	0	0

cannot simulate the effects of the water-vapour phase transition. While some degree of arbitrariness is introduced in the model based on the discretionary value of the threshold, it must be noticed that the effects of the cavitation are negligible for vertical water impacts where the mass effects are dominant and the water spray does not interact with the sphere after the first collision with the water surface.

Conversely, the cavitation plays a relevant role in ditching events. The air-water transition process is a non-steady phenomenon and the continuous formation and collapse of water bubbles has significant effects on the stability of the water flow over the fuselage. A more rigorous modelling approach for the cavitation would include the phase transformation of water from liquid to gas. However, it requires a mesh refinement in the contact zone because the cavitation occurs on a small time and spatial scale.

The air region is not included in the model for the analysis of vertical impacts. This simplification disregards the effects of the air cushion, which is caused by the air entrapped between the body and the water free surface, and it is assumed to have a marginal effect on the impact.

To determine the proper size of the water domain, two phenomena must be considered: the reflection of the pressure waves and the dispersion of surface waves. A non-reflective condition is numerically enforced on the bottom and on all the lateral boundaries of the water tank; this allows to compute a virtual impedance at the interface that prevents the pressure waves to be reflected back inside the domain. Furthermore, the water tank must be large enough such that the surface waves do not interact with the boundaries. While the dispersion velocity of the waves is a function of the ratio between the depth of the water and the wavelength, in shallow water a good approximation is given by [18]

$$v = \sqrt{gh},$$

where g is the gravitational acceleration and h is the depth of water. Therefore, given the time interval of interest, it is possible to estimate the minimum size of the water domain such that the surface waves do not reach to the boundaries.

Another problem shall be considered in case of finite-size fluid domain. If the lateral displacements of the water are constrained, the fluid tends to expand in the vertical direction because of the volume occupied by the sphere. It leads to erroneous results since the actual velocity of penetration of the sphere into water is equal to the algebraic sum of the sphere velocity and the rate of change of the water free surface level. Particular attention is therefore required for small domains where the water level may significantly be influenced by the presence of the sphere. Toso [29] suggests that the width of the water tank should be at least twice the diameter of the sphere. In light of the previous considerations, a 560 mm by 560 mm square water tank with a depth of 250 mm is used for the simulations.

A convergence analysis was performed to determine the optimal size of the elements. It was decided to base the convergence criteria on the mean integral acceleration evaluated in the first 3.5 ms after the impact. From the results of these analyses, four meshes were selected and used as references to compare the differences among the models used for the water,

- In the Lagrangian model, the water mesh is made by 627,200 hexahedral elements.
- In the ALE model, the fluid mesh is made by 878,080 hexahedral elements among which 627,200 represent the water and 250,880 the initial air region.
- In the pure SPH model, the water domain consists of 627,200 discrete particles.
- In the hybrid Lagrangian-SPH model, the water mesh is made of 487,232 hexahedral Lagrangian elements and 139,968 discrete particles. The optimal ratio of SPH particles to Lagrangian elements is 1/8, in terms of volume of water. This value is selected after a series of analysis aimed to obtain the best correlation with the experimental data.

The hexahedral elements used in the Lagrangian, ALE and hybrid models have a constant edge-length of 5 mm. In the SPH and in the hybrid model, the water particles are uniformly distributed and have a smoothing length of 5 mm.

Analysis of the results and discussion

The quantitative comparison of the models is based on the vertical accelerations of the sphere, on the penetrations into the water and on the distribution of the hydrodynamic pressure on the bottom surface of the sphere. The vertical acceleration of the sphere obtained by the numerical analysis is correlated to the experimental data.

The reference experimental value for the first acceleration peak is 64.4 g, while the average acceleration evaluated 10 ms after the impact is 25.3 g. The numerical acceleration is measured on a node located at the top-centre of the sphere. To remove the spurious noise, the raw numerical signal is imported in MATLAB and filtered with a low-pass Butterworth filter with a cut-off frequency of 1 kHz. The correlation of the experimental

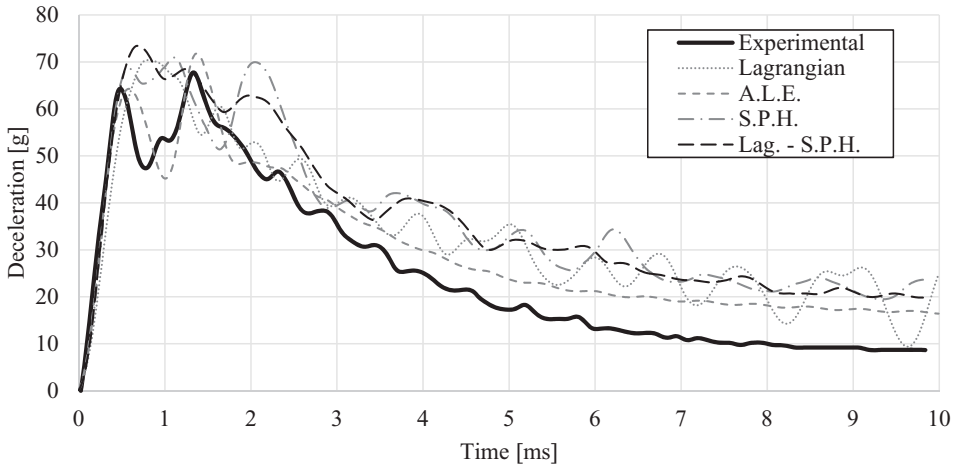

Figure 1. Sphere vertical acceleration: correlation of numerical simulations with experimental data.

and the numerical accelerations is shown in Figure 1. The reference value of penetration into water is 100 mm. It is computed through a double-integration of the given experimental acceleration assuming an initial velocity of 11,800 mm/s and a zero initial distance from the water free surface.

The results of the numerical-experimental correlation are summarised in Table 2. All the percentage differences are computed using the experimental data as reference values. The reported CPU times refer to a simulation time of 15 ms. All the simulations are performed with the commercial code LS-DYNA, version R6.1.1, on a workstation Intel Xeon E5 – 1603 at 2.80 GHz with 16 GB RAM.

All the models over-estimate the average deceleration. To explain the discrepancy with the experimental value, it is worth to consider that the sphere is assumed to be perfectly rigid in the models. However, elastic deformations might have occurred in the experimental test after the first acceleration peak. Indeed, the compliance of the structure is of primary importance in FSI simulations because the hydrodynamic loads depends on the geometry of the structure interacting with the fluid, while the structural deformation depends on the pressure generated at the interface. However, in case of high velocity vertical impacts, the mass effects are dominant compared to the hydrodynamic effects. Therefore, the forces acting on the sphere are proportional to rate of fluid mass displaced by the body while entering the water. If the sphere is rigid, all its initial momentum is transferred to the fluid.

If a non-rigid sphere would be considered, it is reasonable to expect that part of its initial kinetic energy is converted into deformation energy, which may be dissipated due to plastic mechanisms. In this case, both the thickness and the mechanical properties of the material become additional parameters of the analysis, making more difficult to draw general conclusions about the modelling techniques for the fluid domain.

The first acceleration peak is over-estimated by the Lagrangian, the SPH and the hybrid Lagrangian-SPH model respectively by 9.3%, 6.55% and 14%. The ALE model under-estimates the first acceleration peak by 0.2%. The second acceleration peak is predicted by the ALE and the SPH models only. They both over-estimate the magnitude by respectively 6.2% and 3.5% compared to the 67.6 g obtained from the experimental test.

The steady acceleration predicted by the SPH and by the hybrid models is larger than the value obtained from the ALE model because the particle approximation of

Table 2. Correlation of numerical and experimental data of a vertical drop of a rigid sphere into water.

	Elements (water)	Acc. peak (g)	Diff. on peak (%)	Average acc. (g)	Diff. on average acc. (%)	Depth after 10 ms (mm)	Diff. on depth (%)	CPU time
Exp.	–	64.4	–	25.32	–	100	–	–
Lag.	627,200	70.38	9.29	33.76	33.33	97.40	−2.6	3 h 23 min
ALE	627,200	64.27	−0.19	30.49	20.42	99.05	−0.95	1 h 16 min
SPH	627,200	68.62	6.55	36.62	44.63	95.84	−4.16	1 h 33 min
Lag.-SPH	487,232 (Lag.) 139,968 (SPH)	73.43	14.02	36.72	44.94	95.91	−4.09	3 h 41 min

the water domain has a stiffer behaviour compared to the FE approximation. As a result, the penetration predicted by the SPH and by the hybrid model is smaller compared to the result predicted by the ALE model.

The numerical acceleration predicted by the Lagrangian model does not tend to a steady value and the amplitude of the spurious oscillations increases with time. This can be related to the deformation of the elements and to the presence of the hourglass energy in the model.

The deformation of the Lagrangian mesh leads to large distortions in those elements located underneath the bottom of the sphere. By the end of the simulation, their aspect ratio, which is determined by the ratio of the maximum and the minimum distance between any couple of opposite faces, reaches an approximate value of 150 while the optimal value is 1. This introduces inaccuracies in the solution due to the bad integration of the stiffness matrices.

The presence of the hourglass energy can be reduced by refining the mesh. In the convergence analysis, it was found that the percentage of hourglass energy compared to the total energy computed 5 ms after the impact is 13.2%, 7.86% and 6.73%, respectively, by using 10, 5 and 4 mm edge-length elements. However, by reducing the size of the elements, the Lagrangian mesh becomes more sensitive to the time-step reduction caused by distortion of the elements.

The distribution of the hydrodynamic pressure on the bottom surface of the sphere is used to compare the differences between the four formulations on a local scale. Two different approaches are used to measure the pressure acting on the sphere.

In the ALE model, the pressure is computed from the coupling forces acting between the fluid and the structure mesh. Virtual pressure gauges are defined on selected elements of the sphere and the pressure is measured at the centroid of these elements. In both the Lagrangian and in the SPH models, the pressure is obtained from the contact forces between the sphere and the water which are measured at the nodes of the sphere. The pressure acting on each virtual gauge is then obtained by averaging the pressures at the four nodes of the corresponding element.

The distribution of the virtual gauges on the sphere is shown in Figure 2. In order to obtain a good spatial resolution, 27 virtual gauges are distributed on the *xz* symmetry plane of the sphere. The sensors are evenly arranged around the central element which lies also on the *yz* symmetry plane. A MATLAB script was created to generate the list of virtual sensors which is then included into the LS-DYNA models. The pressure is sampled at 10 kHz. The numerical signal is imported in MATLAB and filtered through a low-pass Butterworth filter with a cut-off frequency of 5 kHz. The pressure distributions obtained from the four simulations are shown in Figure 3 by using iso-pressure contour plots. The horizontal axis represents the simulation time while the vertical axis indicates the distance from the centre of the sphere. A vertical reading represents the distribution of the pressure over the sphere at a specific time, a horizontal reading represents the pressure history at a specific point on the surface of the sphere. The plots are reported on the same pressure scale and the time axis is limited to the first 3 ms after the impact.

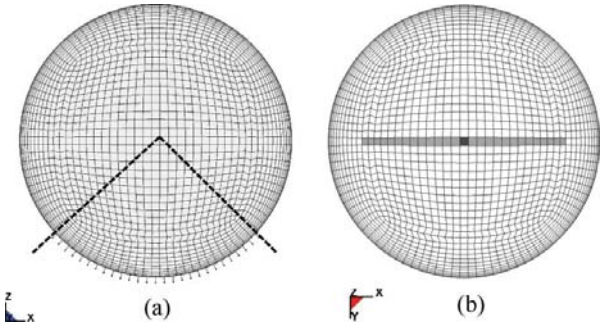

Figure 2. Distribution of virtual pressure gauges on the sphere: (a) side and (b) bottom view.

The distribution of the hydrodynamic pressure obtained from Lagrangian and ALE models is expected to be a smooth function of the spatial coordinate because these formulations represent continuous approximations of the fluid domain. Discontinuities in the pressure field along the spatial direction are related to the sampling procedure which is based on discrete readings over the surface of the sphere. Conversely, the pressure distributions obtained from the SPH and from the hybrid models are less smooth along the spatial coordinate because of the discrete nature of the particle formulation. As expected, all the models predict a pressure distribution which is symmetric about the centre of the sphere.

All the models show an initial peak in the pressure caused by the impact of the sphere on the water surface. The peak, which is initially located at the centre of the sphere, decreases in intensity while spreading towards the sides as long as the sphere penetrates into the water. The distribution of the hydrodynamic pressure is correlated with the acceleration of the sphere. The result obtained from the Lagrangian model shows oscillations in the pressure distribution starting 1 ms after the impact. These oscillation matches with the spurious peaks of the acceleration signal reported in Figure 1. The result of the ALE model shows a second overpressure peak in the time interval between 1 and 1.5 ms after the

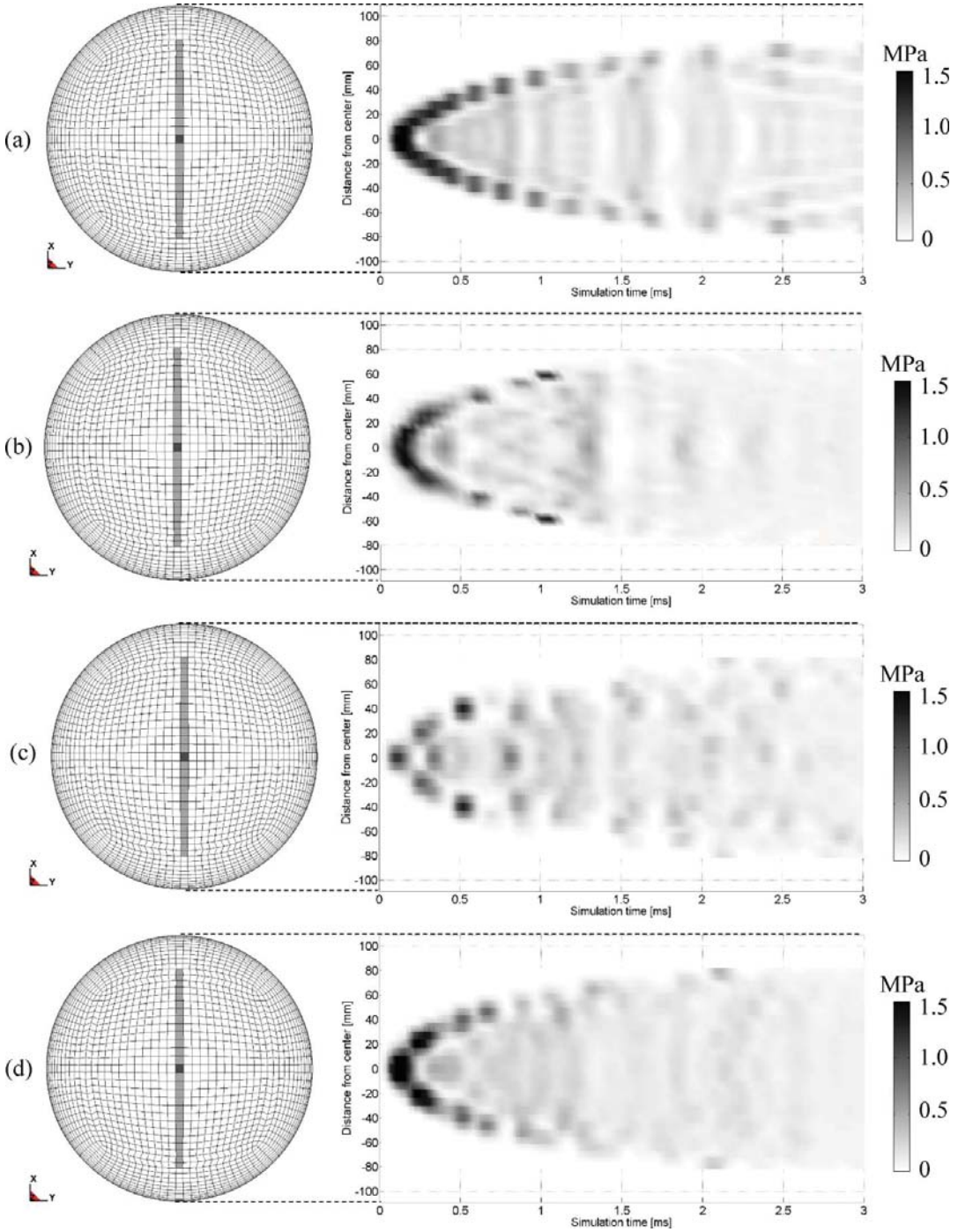

Figure 3. Pressure distribution over sphere bottom surface: (a) Lagrangian, (b) ALE, (c) SPH and (d) hybrid Lagrangian-SPH.

impact, which corresponds to the second acceleration peak. Conversely, except for the first peak, there is no significant correlation between the pressure distributions predicted by the SPH and by the hybrid model and the corresponding acceleration signals.

The impact sequence predicted by the ALE model is reported in Figure 4 along with the sphere vertical acceleration. In the initial stage, the water response is linear and the first acceleration peak is related to the water compressibility. The first peak is followed by a sudden drop in the acceleration. The second image represents the time of the second peak. The development of a surface wave can be observed around the sphere. The third picture represents an advanced stage of the impact

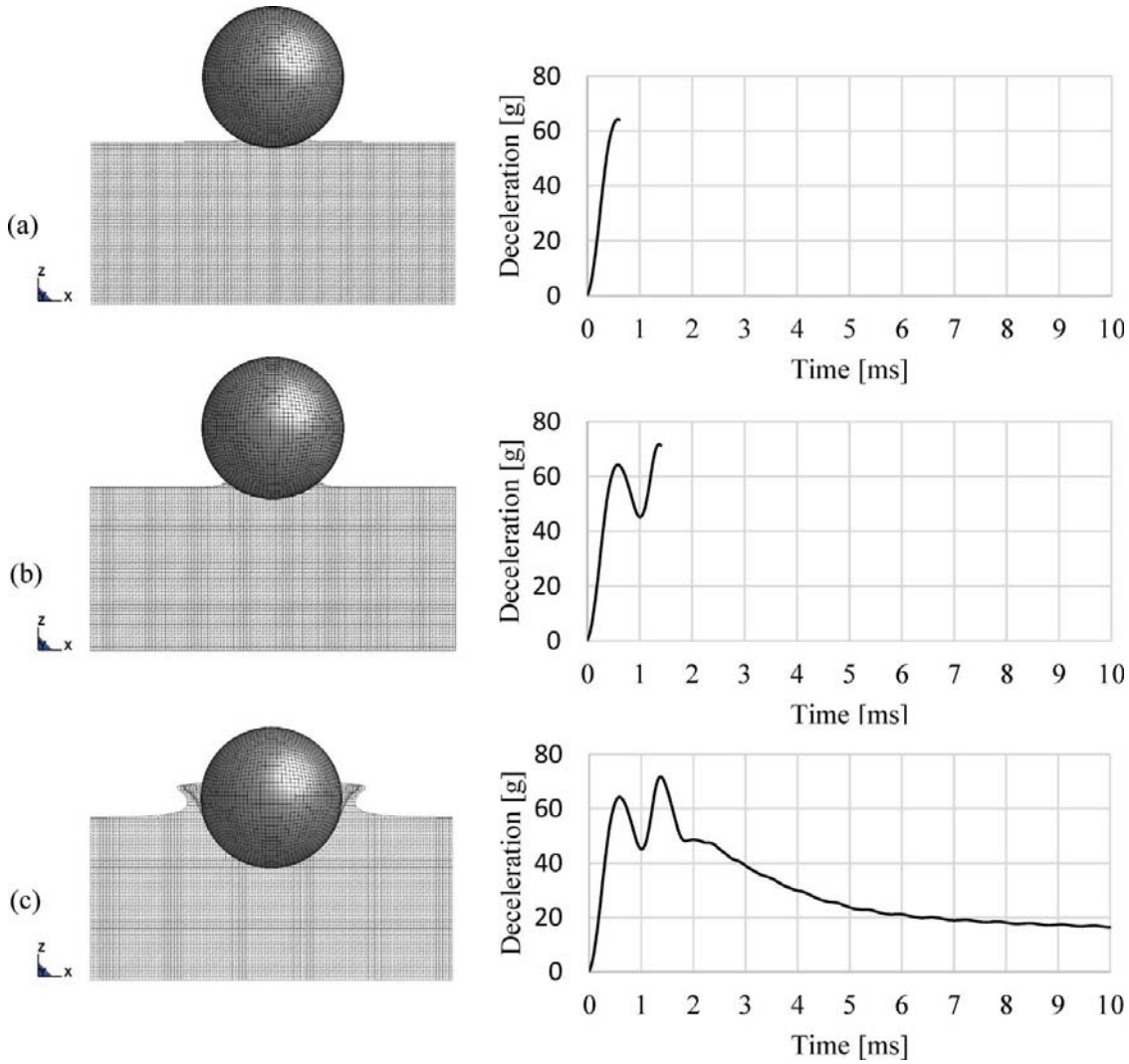

Figure 4. Sphere impact predicted by ALE model: (a) 0.75 ms, (b) 1.6 ms and (c) 10 ms after impact.

when the sphere is partially submerged. The buoyancy force becomes relevant and the acceleration decreases smoothly to a steady value. The surface wave is no longer in contact with the sphere and its tip is separating to create the water spray.

The cut-off sections of the water domains, shown in Figure 5 at 10 ms after the impact of the sphere, allow to compare the behaviour of the different formulations when the fluid is subjected to large deformations. The Lagrangian model does not predict the separation of the water spray and the water exhibits a stiffer behaviour compared to the other models. Because of the extreme deformation of the elements, the mesh results locked in the closeness of the spray tip which does not collapse under the effect of the gravity. In the ALE model, the water flows through the mesh and the accuracy of the results is not affected by the deformation of the water domain.

The SPH and the hybrid model predict similar results. Looking at the SPH water model, it can be observed that a large part of the fluid domain, in the closeness of the boundaries, is not deformed by the presence of the sphere at the end of the simulation. This justifies the adoption of the hybrid Lagrangian-SPH water model to reduce the number of particles. Despite the discontinuity introduced by the hybrid formulation, the coupling algorithm between the Lagrangian mesh and the SPH elements allows to transfer the impact pressure. The deformation of the water domain is continuous and the slope of the surface is preserved across the discontinuity. The concentrated loads introduced by the SPH particles lead to large deformations of Lagrangian elements at the

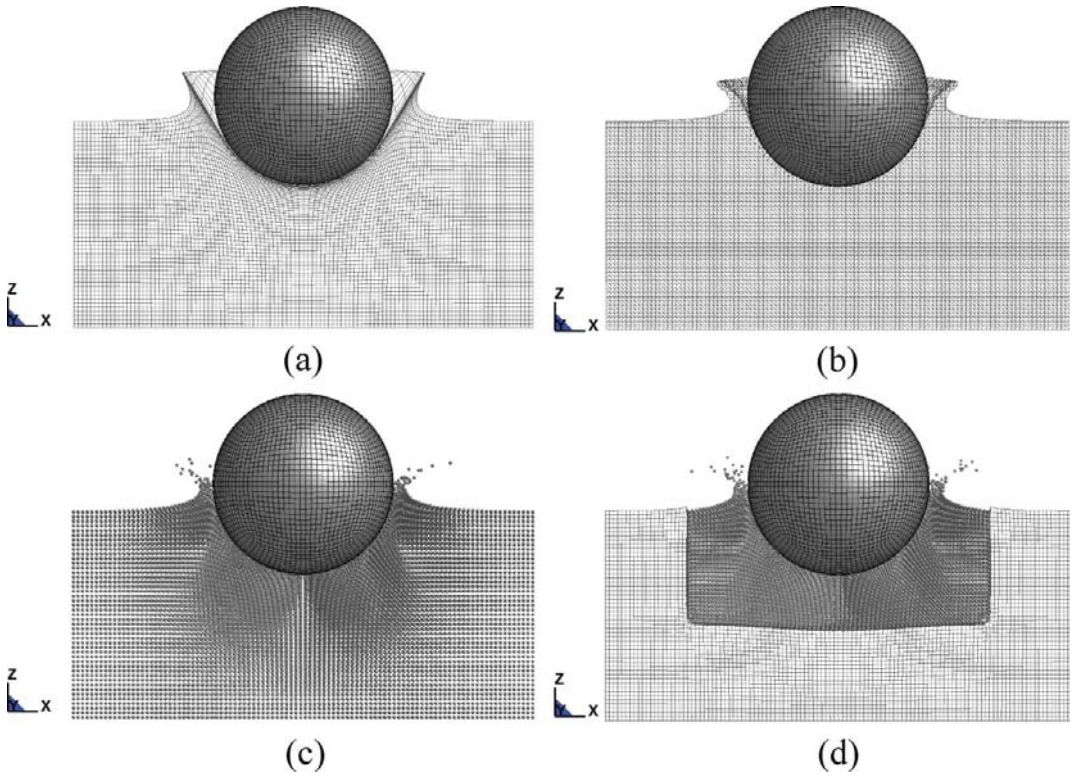

Figure 5. Comparison of different water formulations at $t = 10$ ms: (a) Lagrangian, (b) ALE, (c) SPH and (d) hybrid Lagrangian-SPH.

bottom interface. This local instability causes the reduction of the time step and the increase of the hourglass energy.

In addition to the quantitative comparison between the models, these analyses allow to draw further considerations about the formulations and the different modelling techniques.

By comparing models with the same number of elements, it is found that the Lagrangian formulation is not competitive in terms of CPU time compared to the ALE and to the SPH methods for those problems related to large deformations of the fluid domain. Indeed, the Lagrangian mesh suffers from the reduction of the analysis time-step caused by the progressive distortion of the elements. This limitation affects both the purely Lagrangian and the hybrid model.

In the pure Lagrangian model, the elements located on the surface impacted by the sphere are progressively compressed and thinned. As a result, the time step is reduced by a factor of 40 by the end of the analysis. A possible solution to this inconvenient would be to create a mesh made of elements stretched in the direction of the velocity vector of the sphere, such that the elements would naturally tend to a cubic shape while deforming under the impact load. This strategy is applicable only if the deformation field of water is known in advance. Conversely, the problem of the hybrid model is related to the local effects at the interface between the Lagrangian mesh and the SPH particles, where the Lagrangian elements result excessively distorted because of concentrated loads introduced by the penalty coupling forces. In the hybrid model the edge-length of Lagrangian elements is equal to the dimension of the SPH particles. However, it is found that the deformations of the Lagrangian mesh at the interface can be significantly reduced by increasing the edge-length of the Lagrangian elements up to 1.5 times the dimension of the SPH particles. This solution allows to increase the computational performance by preventing the time-step reduction related to the local instabilities of the Lagrangian mesh.

Another peculiar problem related to the discrete SPH method is the artificial dissipation introduced by the Monaghan artificial viscosity. If added to the model, the energy ratio computed after 10 ms of analysis is equal to 0.778, while the energy ratio is 0.998 if the standard viscosity is used. A lower ratio indicates that a large amount of energy is numerically dissipated from the system. While the Monaghan viscosity allows to stabilise the solution in case of high-speed impacts, for low-speed FSI problems the standard formulation for viscosity is preferred.

Table 3. Scale relationships based on the Froude number similarity.

		Scale factor			
	Model	1/30	1/20	1/15	1/10
Length (m)	1.22	36.58	24.38	18.29	12.19
Mass (kg)	5.67	153,090	45,360	19,136	5670
Velocity (m/s)					
Hor.	9.14	50.08	40.89	35.41	28.92
Vert.	0.20	1.10	0.89	0.77	0.63

Ditching of a rigid airplane

Two numerical simulations of a representative ditching of a simplified airplane are conducted. The loads acting on the fuselage during a controlled landing on calm water are evaluated. These simulations allow to compare the computational performances and the accuracy of two different modelling techniques for fluids domains in the framework of non-vertical FSI impact problems.

The simulations are based on an experimental test conducted by NACA [19] aimed to assess the response of a generic scale-size airplane during a controlled landing on water. According to the scaling law based on the Froude number similarity, the results obtained from these simulations can be extended to a wide range of full-scale ditching scenarios. For example, by assuming a scale factor of 1/20 as reported in Table 3, the results obtained from the simulation of the scaled aircraft are representative of a ditching of a twin-engine small commercial jet airliner.

Compared to vertical impacts on water, ditching phenomena are more difficult to be simulated because the horizontal velocity of the airplane generates complex hydrodynamic phenomena such as the suction, the cavitation, the cushioning effect and the ventilation [16].

Following the results obtained from the vertical impact simulations, two different modelling approaches are adopted to represent the water domain. In the first model the water is represented by means of an Eulerian mesh and the FSI interaction is simulated through an ALE method. In the second model, the water is represented by means of a hybrid Lagrangian-SPH formulation.

Description of the models

The FE model of the scaled airplane, shown in Figure 6, is developed following the specifications provided in the NACA's technical report. Two major simplifications are adopted: the aerodynamics effects are disregarded and the airplane is assumed to be perfectly rigid.

The latter assumption is partially justified by considering that the test article did not report permanent damages during the experimental campaign. Also, not enough information can be found in the report for the estimation of the elastic properties of the airplane.

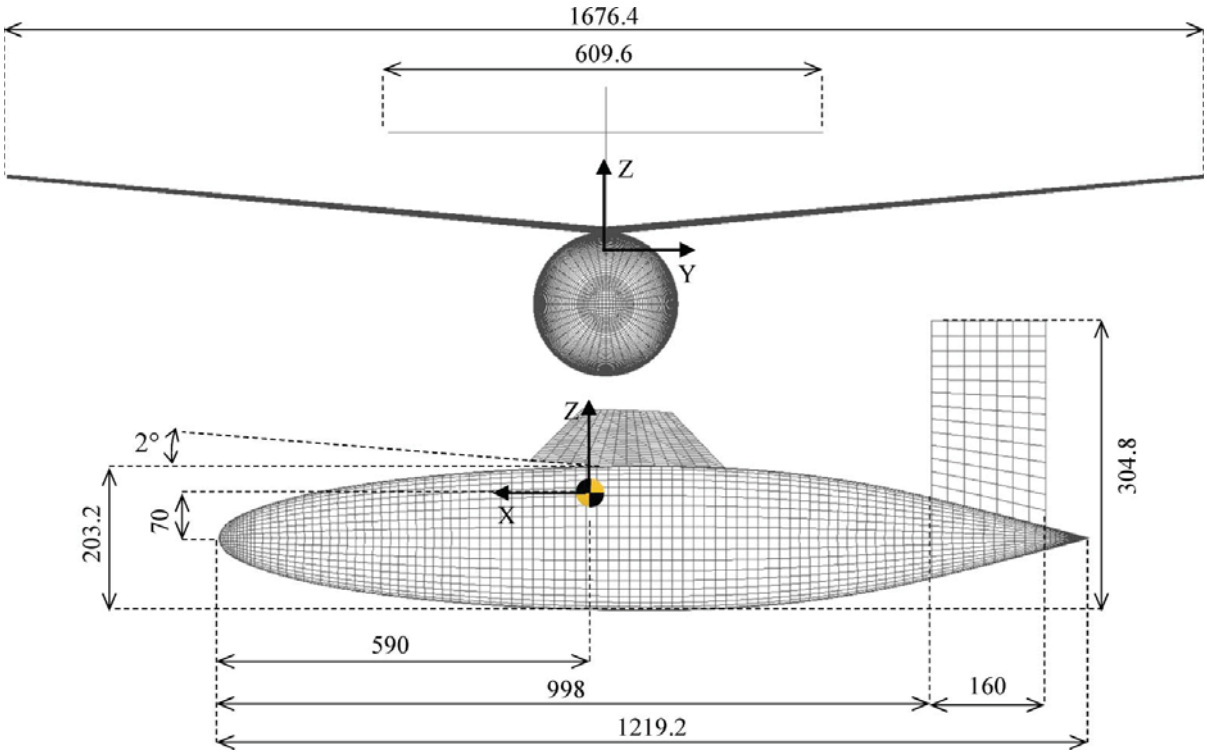

Figure 6. Airplane FE model and local coordinate system (dimensions in mm).

Table 4. Inertial properties of NACA airplane.

Distance of CoM in local coord. sys.			Moment of inertia about CoM		
x (mm)	*y* (mm)	*z* (mm)	Roll (kg*m^2)	Pitch (kg*m^2)	Yaw (kg*m^2)
590	0	70	0.541	0.293	0.748

The fuselage is modelled as an axisymmetric surface, the profile of the fuselage is obtained through a spline interpolation of the point coordinates reported in [19]. The nose-tip distance is 1219.2 mm and the maximum width is 203.2 mm. The wing and the tail stabilisers are represented by flat surfaces because the aerodynamics effects are neglected. The airplane is modelled with a rigid-type material and is discretised with 4911 Lagrangian quad-node shell-type elements.

The mass of the entire aircraft is 5.67 kg while the centre of mass (CoM) is located at 30% of the mean aerodynamic chord and 70 mm above the centreline of the fuselage. The model is divided into five parts and their thicknesses are determined in order to match the mass and the moment of inertia about the pitch axis of the original NACA airplane. The inertial properties of the FE model are summarised in Table 4.

The initial horizontal velocity is 9144 mm/s and the attitude is 10°, which is the high-nose angle recommended for ditching. The initial descending rate is assumed to be equal to 200 mm/s. Since this data is omitted by NACA, a reasonable assumption was made by considering that the maximum vertical speed in a controlled ditching of a full-scale airplane is 1.5 m/s [16]. This value is scaled according to the Froude number similarity by assuming that the equivalent forward velocity is equal to 64.3 m/s, which is a reference ditching speed [21].

The water region included in the models is 3200 mm long, 800 mm wide and 350 mm deep. These dimensions were defined after a series of preliminary analysis aimed to verify that the results are not affected by boundary effects. The fluid-structure coupling is enforced by mean of frictionless penalty contacts. In order to simplify the model, the interaction of the horizontal stabiliser with water is disregarded because, in the experimental tests, it is designed to separate from the fuselage as soon as it comes in contact with water.

The ALE model includes an air region above fluid domain. However, the aerodynamics forces and the interaction of the fuselage with the surrounding air are disregarded in the analyses. This is considered a conservative simplification because the lift force and the cushioning effect are expected to reduce the loads acting on the fuselage

The water is represented by 882,000 hexahedral elements. The air volume, which is of the same size of the water region, is made of 441,000 hexahedral elements. In order to limit the number of elements, the mesh is refined in the contact zone where the average edge-length is 6.7 mm.

The air and the water are in equilibrium state at the beginning of the simulation and the initial pressure is set to 101,325 Pa which is the atmospheric pressure at the sea level. This offset is introduced to simulate the effects of low pressure zones. If the reference pressure is set to zero, the simplified cut-off cavitation algorithm erodes the elements and the model cannot simulate the suction effect.

The hybrid Lagrangian-SPH water is made by 1,560,000 particles with a size of 6 mm and 559,040 hexahedral elements with an edge-length of 10 mm. A section of the hybrid water model is shown in Figure 7. The SPH elements, which are evenly distributed in the entire domain, represent 38.6% of water cross-sectional area. The Monaghan artificial viscosity is not included in the model.

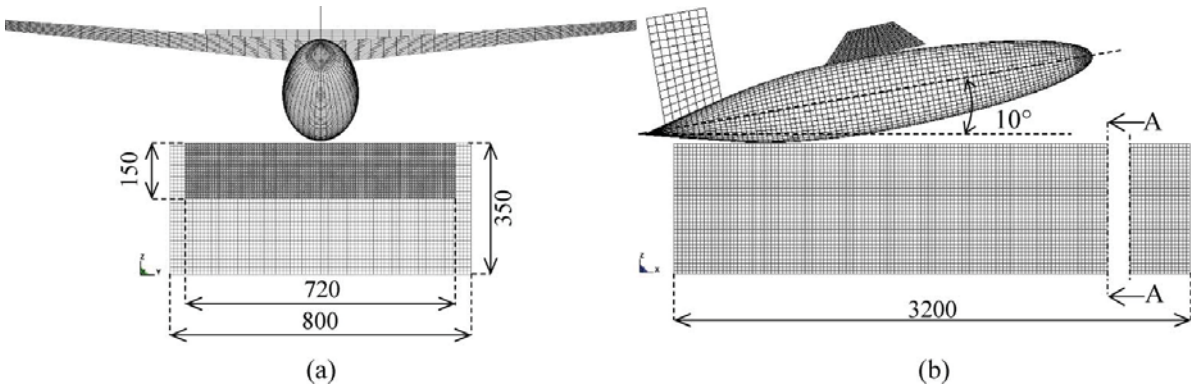

Figure 7. Lagrangian-SPH model: (a) A-A section view and (b) lateral view (dimensions in mm).

Table 5. Linear polynomial EOS coefficients for ditching simulations.

Material	C_0 (MPa)	C_1 (MPa)	C_2 (MPa)	C_3 (MPa)	C_4	C_5	C_6
Water (ALE)	0.101325	2723	7727	14,660	0	0	0
Water (Lag.-SPH)	0	2723	7727	14,660	0	0	0
Air	0.101325	0	0	0	0.4	0.4	0

Two linear polynomial EOS associated to a null-type material are defined for the water and the air. The EOS coefficients are reported in Table 5. The initial reference pressure for the ALE model is imposed equal to 1 atm by setting C_0 = 0.101325 MPa. Since the SPH formulation that is currently implemented in LS-DYNA cannot simulate the suctions forces, the reference pressure is set equal to zero in the hybrid model. The slippery condition is imposed on all the sides and on the bottom boundaries of the water mesh.

Analysis of the results

A representative ditching scenario is simulated. The airplane horizontal velocity and the attitude angle obtained from the simulations are used to validate the models through the correlation with the experimental data. The correlations are reported in Figures 8 and 9, respectively. The numerical data are obtained as nodal outputs from a node located at the CoM of the airplane and are expressed in the global reference coordinate system. The experimental data are taken from literature [19].

The variation of the horizontal velocity is mainly related to the transfer of momentum from the airplane to water via hydrodynamic effects. Since the FSI is enforced through an algorithm, which ensures the conservation of the momentum, the accuracy of the correlation is related to the capabilities of the models to

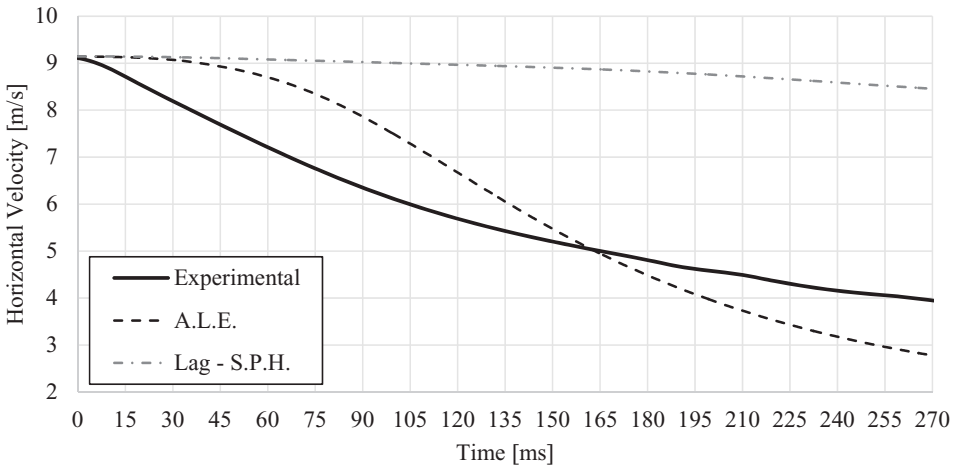

Figure 8. Airplane horizontal velocity computed at CoM in global coordinate system.

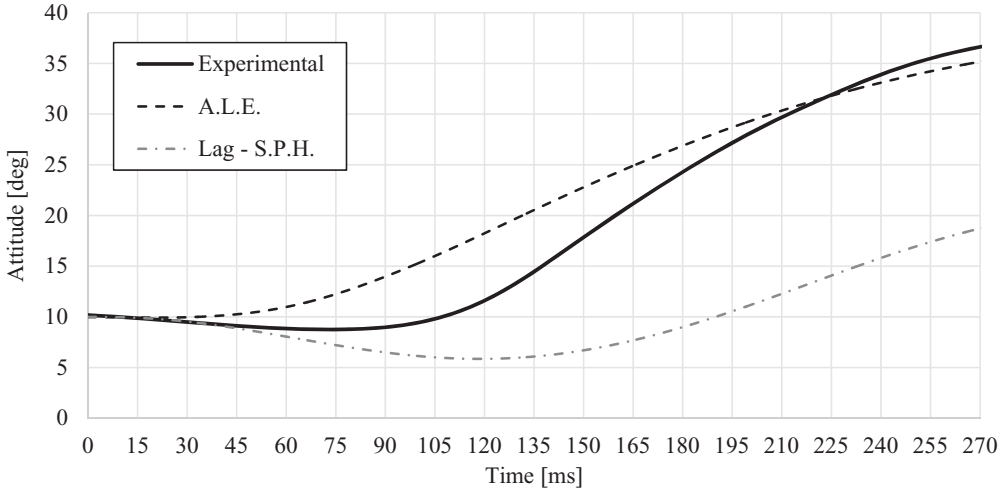

Figure 9. Airplane attitude angle.

simulate hydrodynamic phenomena. In the initial stage of the simulation, both models underestimate the reduction of the velocity because they cannot simulate the tangential forces due to the viscous friction between the fuselage and the water. Indeed, the coupling forces between the Eulerian and the Lagrangian elements act perpendicularly to the fuselage surface. While the simulation advances, the differences between the ALE and the hybrid models become relevant. The suction forces in the ALE models cause the fuselage to sink and the attitude angle to increase significantly compared to the hybrid model. These effects lead to a larger drag force acting on the fuselage and, by the end of the simulation, the differences between the numerical and the experimental velocity are −29.6% and 114.2% for the ALE and for the hybrid model, respectively.

The variation of the attitude angle is related to the inertial and to hydrodynamic effects. As shown in Figure 9, the experimental attitude angle decreases in the initial stage of the ditching, when inertial effects are dominant. Since the aircraft impacts the water surface with an initial nose-up attitude, the impact pressure acting on the aft of the fuselage leads to an unbalanced pitch moment that causes a nose-down rotation of the aircraft. In a second stage, the hydrodynamic effects become relevant and the pitch moment caused by the pressure distribution acting on the fuselage results in a nose-up rotation.

In the ALE model, the inertial effect is limited to the first 30 ms after the contact with the water surface, while the low pressure acting on the fuselage aft causes the attitude angle to increase earlier compared to the experimental test. Since the interaction of the airplane with the air is disregarded, the model cannot simulate the ventilation effect which facilitates the separation of the water layer from the fuselage. It results in the overestimation of the suction effects. Conversely, the kinematic of the hybrid model is governed by the inertia. The SPH formulation adopted for the simulation suffers from numerical instability when the particles undergoes to dilatational stresses. Therefore, the hybrid model cannot simulate the effects of the pulling forces between the water and the fuselage in the low pressure zone. The increment in the attitude angle is caused by the overpressure zone acting on fuselage. By the end of the simulation, the difference between the experimental attitude and the prediction is −4% and −48.9%, respectively.

Despite the ALE model of water overestimates the suction effect, by the end of the simulation the experimental attitude angle is larger compared to the prediction. A possible explanation is that, in the experimental test, the horizontal stabiliser separates from the fuselage as soon as it comes in contact with the water. Therefore, the airplane configuration becomes unstable and the aerodynamics generates a nose-up pitch moment while the attitude increases. Conversely, the aerodynamics is disregarded in the numerical model.

The longitudinal and the vertical accelerations of the airplane computed at CoM in the local coordinate system are reported in Figure 10. The numerical data are filtered with a 60 Hz low-pass Butterworth filter. The initial acceleration values are equal to the component of the gravity in the local coordinate system. In the initial

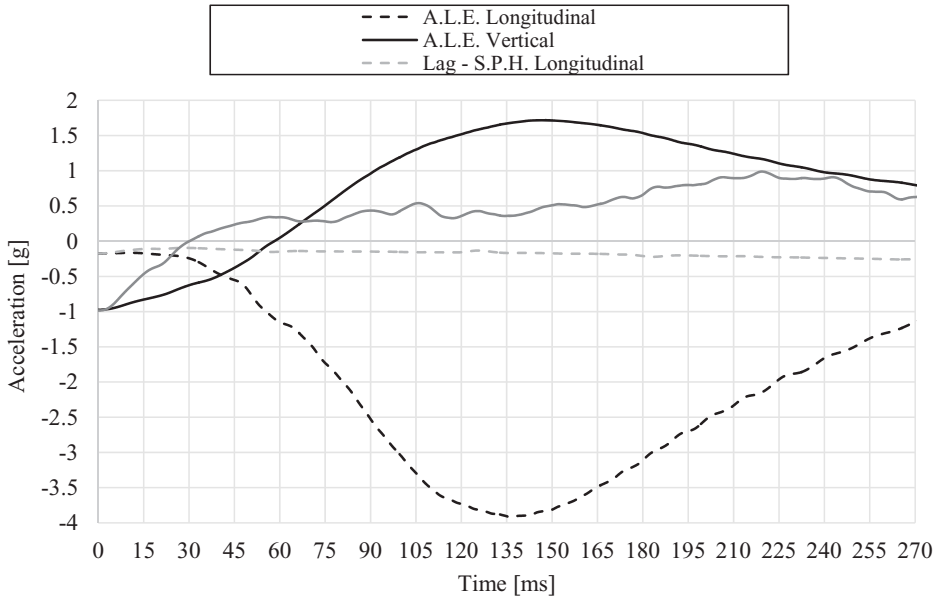

Figure 10. Airplane accelerations computed at CoM in local coordinate system.

stage of ditching, the hydrodynamic effects are negligible and the FSI is dominated by the mass effects. The accelerations are related to the transfer of momentum between the fuselage and the water which occurs in a similar way of purely vertical impacts. As observed in the impacting sphere simulations, the SPH water model is stiffer compared to the FE water and the vertical acceleration predicted by the hybrid model is larger in the first 70 ms after the impact. While the simulations advance, the hydrodynamic effects arise and become dominant over the mass effects.

The vertical acceleration of the ALE model grows smoothly from the initial value of −1 g to a peak of 1.76 g that is reached 145 ms after the first impact. Then, the deceleration decreases smoothly reaching a value of 0.8 g by the end of the simulation. The SPH approximation adopted in the hybrid model leads to a noisier acceleration history compared to the result of the ALE model. The high frequency variations in the signal are caused by local collisions of the water particles on the fuselage. After the initial stage, the vertical acceleration exhibits a slow and non-monotonic growth until it reaches a peak of 0.98 g approximately 220 ms after the first impact. At the end of the simulation, the vertical acceleration is equal to 0.68 g.

The longitudinal accelerations obtained from the numerical simulations do not change in sign, which means that they are always oriented from the nose toward the aft of the fuselage. However, the differences between the models are more pronounced compared to the vertical accelerations. The magnitude predicted by the ALE model smoothly increases in modulus from an initial value of −0.17 g to a peak of −3.92 g which is reached 135 ms after the initial contact. The acceleration decreases monotonically after the peak and reaches a value of −1.45 g by the end of the simulation. The longitudinal acceleration obtained from the hybrid model is almost constant during the entire simulation and the variation range is limited between 0.079 g and −0.084 g with respect of the initial value which is equal to −0.17 g.

The pressure data are obtained from 27 virtual gauges distributed along the symmetry plane of the aircraft, as shown in Figure 11. Each virtual gage is made by two identical elements and the pressure is computed by averaging the value computed on both elements. The numerical data are sampled with a frequency of 10 kHz and the raw signals are filtered with a 180 Hz low-pass Butterworth filter.

The distributions of the hydrodynamic pressure on the bottom surface of the fuselage are shown in Figure 11 by using iso-pressure contour plots. The pressure reported in the plots is obtained by scaling the initial equilibrium pressure from the actual values obtained from the simulations. The marked trace in the plots represents the evolution in the space and in the time coordinates of the pressure peak generated by the first contact between the fuselage and the water surface. In both models, the magnitude of the pressure peak, which is initially located in the closeness of the fuselage aft, increases while the position of the peaks moves toward the airplane nose.

According to the prediction of the ALE model, the width of the initial peak, measured along the fuselage symmetry axis, increases with time. The peak reaches the position of the CoM where it stabilises for 100 ms before its magnitude suddenly decreases to zero. The vanishing of the pressure peak corresponds to the generation of a stable wave in front of the fuselage. The low pressure zone, which is visible in the results predicted by the ALE model, is limited in time from 30 to 100 ms after the first contact.

The peak predicted by the hybrid model moves toward the nose of the fuselage and goes beyond the position of the CoM. This effect, combined with the gravity, generates a nose-up pitch moment which causes the attitude angle to increase even without the action of the pulling forces related to the suction. By the end of the simulation, the pressure peak does not vanish but spreads along the fuselage.

It is worth to recall that both the models are conservative. The accelerations and the pressure distribution obtained from the simulations do not take into account for the cushioning effect, caused by the trapped air between the fuselage and the water free surface, which alleviates the loads acting on the fuselage by increasing the duration and by reducing the magnitude of the pressure peaks.

A sequence of the simulated ditching is shown in Figure 12 for both the ALE and the hybrid Lagrangian-SPH model. The airplane impacts the water surface after 15 ms of simulation time. The first image is taken 35 ms after the first impact and represents the end of the initial stage, when the hydrodynamic phenomena begin to develop. By this time, the horizontal velocity predicted by the ALE model is 2.5% smaller compared to the hybrid model, while the attitude is 21% larger. The second image in the sequence is taken 135 ms after the initial contact when the vertical acceleration predicted by the ALE model reaches its maximum. At this stage, the differences between the models are more pronounced. In the ALE model the fuselage is partially submerged while the water flows around without separation. No water spray is observed. Conversely, in the hybrid model the fuselage is completely emerged and the water flow separates from the fuselage generating spray. The last

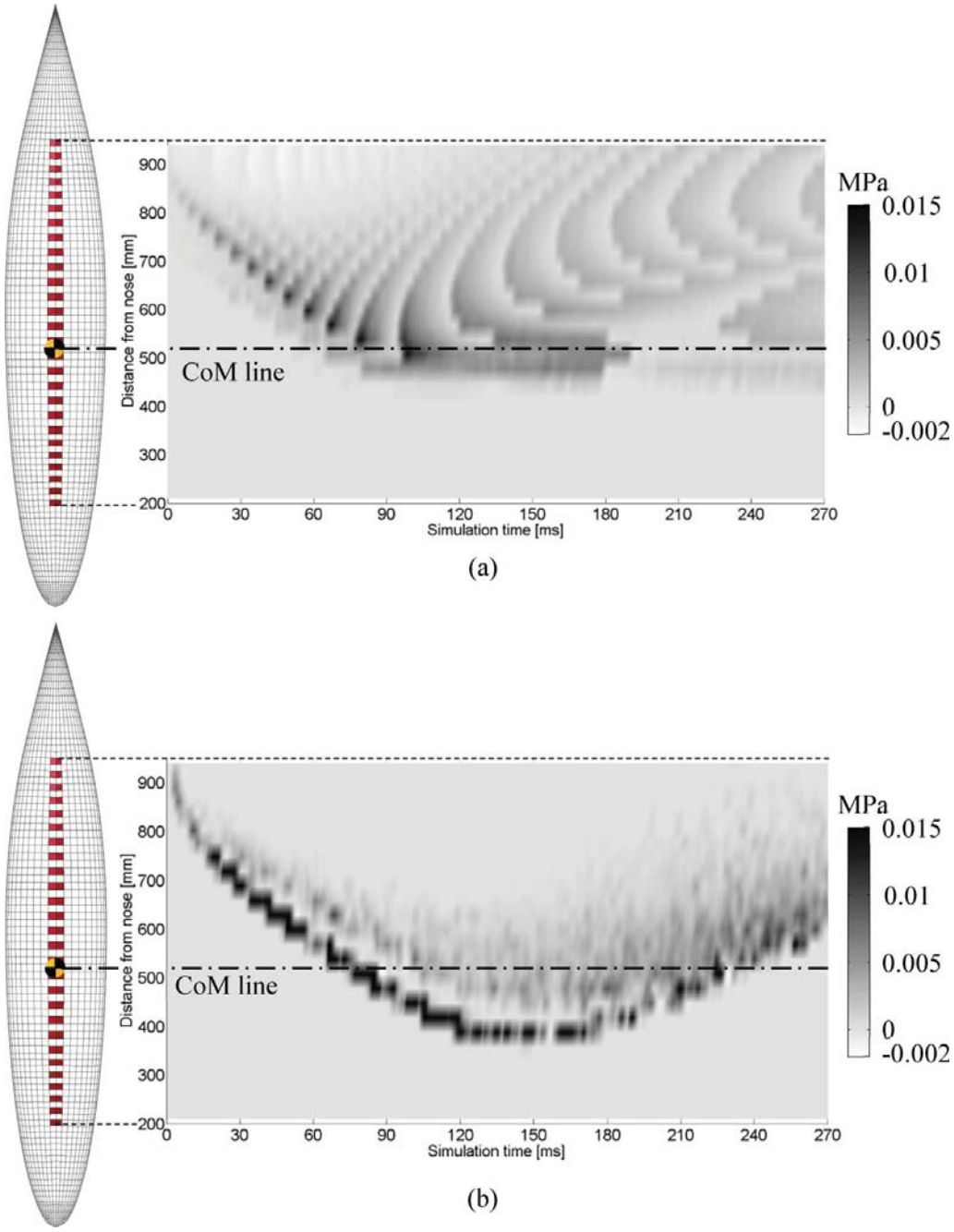

Figure 11. Pressure distribution on fuselage bottom: (a) ALE model and (b) hybrid Lagrangian-SPH model.

image is taken after 250 ms of simulation time. Both the ALE and the hybrid models predict that, by the end of the simulation, the airplane does not bounce on the water surface and the wing does not come in contact with water. In the ALE model, the airplane exhibits a pronounced nose-up trim and a wave develops in front of the fuselage. The aft of the fuselage results completely submerged but the horizontal stabiliser does not interact with the water. Conversely, the hybrid model predicts a smaller attitude angle and the airplane results only partially submerged because there are no suction forces acting on the fuselage. No wave can be observed in front of the fuselage. Since the SPH model underestimates the longitudinal forces acting on the fuselage, the airplane is closer to the edge of the water domain by the end of the simulation.

The kinematics of ditching is symmetric with respect to the symmetry plane of the aircraft because the hydrodynamic pressure induced by the FSI does not generate any roll or yaw moment on the fuselage.

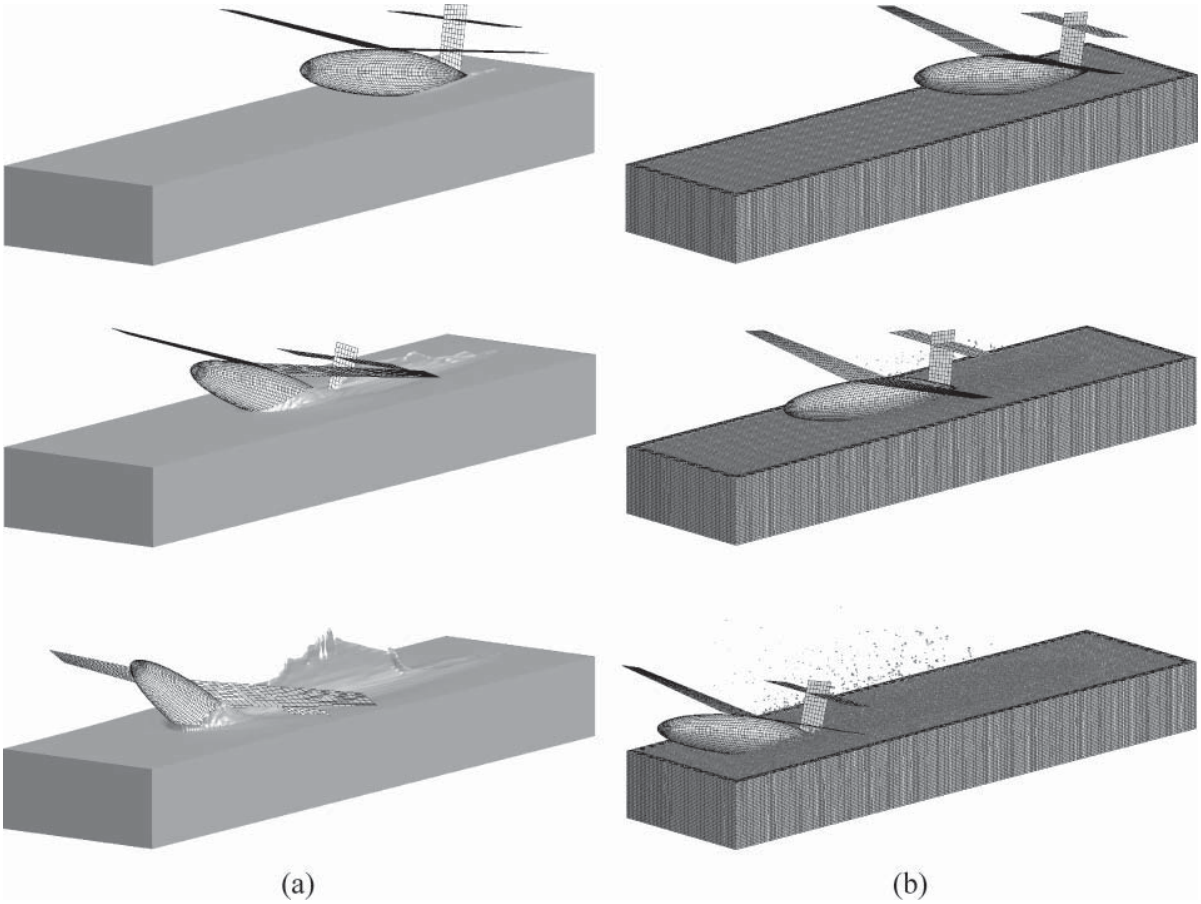

Figure 12. Simulations of ditching at t = 50,150 and 250 ms: (a) ALE model and (b) hybrid Lagrangian-SPH model.

The CPU time required for 270 ms of simulation is 17 h for the ALE and 62 h for the hybrid model on a workstation Intel Xeon E5 – 1603 at 2.80 GHz with 16 GB RAM.

Summary of modelling techniques for fluid-structure interaction

The simulation of a vertical impact on water poses different modelling challenges compared to the simulation of a ditching event. The most important differences are summarised in Table 6. It is also worth to recall that all the analyses presented in this work are based on the assumption that the structure is infinitely rigid.

The advantages and the disadvantages of all the proposed numerical techniques are collected in Table 7. While the optimal modelling strategy depends on the specific problem to be investigated and on the objectives of the analysis, the ALE technique emerges as the most accurate and efficient formulation for both vertical impact and ditching simulations. The use of a pure Lagrangian approach is not advisable because the

Table 6. Differences between vertical water impact and ditching simulations

Vertical impact on water	Ditching
• The impact velocity is perpendicular to the water surface. The horizontal velocity is negligible or null. • The hydrodynamic forces are primarily related to the rate of fluid mass displaced by the object during the impact. • The mass effects are dominant compared to the hydrodynamic phenomena. • The air cushioning effect should be considered for high speed water impact simulations. Disregarding the air trapped between the structure and the fluid surface is considered a conservative approach.	• The vertical component of the impact velocity is small compared to the horizontal component. • The fluid-structure interaction forces are primarily related to the hydrodynamic effects which arise due to the tangential relative velocity. • The mass effects are dominant in the initial stage of the ditching. • The hydrodynamic phenomena such as cavitation, suction and water spray become dominant while the vertical velocity decreases. • The suction force plays a primary role in ditching and so it is decisive to be able to correctly model its effects. • The aerodynamics effects, such as the ventilation and the cushioning which occurs at fluid-structure interface and the lift/drag on the wing, should be considered for high speed ditching simulations.

Table 7. Comparison of the modelling strategies for water impact and ditching simulation

	Analysis	Advantages of the formulation	Disadvantages of the formulation
Lag.	Vertical impact	• Resulting computationally efficient only if the fluid is not subjected to large deformations; • Obtaining accurate results in terms of the initial deceleration; • Not requiring to capture the fluid-structure interface; • Allowing enforcing the fluid-structure interaction by means of penalty contact forces.	• Resulting computationally expensive due to the reduction of the integration time step cause by the mesh distortion; • Suffering from numerical instabilities caused by mesh distortion; • Failing to capture the water spray phenomenon.
ALE	Vertical impact Ditching	• Obtaining accurate results; • Simulating correctly the effect of the suction forces; • Not affecting by numerical instabilities caused by mesh distortion.	• Presenting difficulties to accurately capture the fluid-structure interface;
SPH	Vertical impact	• Not affecting by numerical instabilities caused by mesh distortion; • Allowing to simulate accurately the water spray.	• Resulting computationally expensive; • Requiring a uniform distribution of SPH elements for the discretisation of the fluid domain; • Forcing to introduce numerical viscosity in order to stabilise the analysis in case of high speed impacts; • Suffering from tensile instability and cannot simulate suction.
Lag - SPH	Vertical impact Ditching	• Allowing overcoming the requirement of a uniform distribution of SPH elements; • Requiring a fine SPH discretisation only in the water subdomain where hydrodynamics phenomena of fluid-structure interaction take place.	• Increasing sensitivity of the results, and of the computational efficiency, with respect to the subdivision of the fluid domain in terms of Lagrangian and SPH elements; • Requiring to define additional contact interfaces between the Lagrangian and the SPH elements; • Making difficult to determine a priori the optimal subdivision of the fluid domain in terms of Lagrangian and SPH elements.

distortion of the mesh elements causes numerical instabilities and the reduction of the integration time-step, which deteriorates the efficiency of the Lagragian approach. The SPH method provides accurate results for the high velocity vertical impact simulation, where the mass effects are dominant over the hydrodynamics phenomena. Compared to the ALE, the SPH method is computational more expensive and it requires a uniform discretisation of the fluid domain, while a local refinement is advisable in the area of the fluid-structure interface in order to capture the small-scale hydrodynamics effects. The hybrid Lagrangian-SPH approach allows to overcome this limitation. However, it requires additional modelling efforts in order to determine the optimal subdivision of the fluid volume into Lagrangian and SPH subdomains. In addition, it requires to introduce contact interfaces between the SPH particles and the Lagrangian elements, which may significantly reduce the computational performances of the hybrid approach, eroding its advantages compared to the pure SPH method.

Conclusions

The vertical impact of a rigid sphere into water is simulated in the first part of the paper by using the commercial FE explicit solver LS-DYNA. The objective is the comparison of the formulations available to model water in FSI problems. The results obtained by using the ALE method show the best correlation with the experimental data. The computational performance of the SPH formulation can be improved by replacing part of the fluid domain with Lagrangian elements, while the results from the purely Lagrangian model are affected by the locking of the mesh and by the presence of an excessive amount of hourglass energy.

The low speed ditching of a scaled rigid airplane is presented in the second part of the paper. The models are validated through the comparison with experimental data from literature. The correlation is based on two global quantities: the horizontal velocity and the attitude angle. The airplane accelerations are used to compare the loading conditions predicted in case of ditching. The distribution of the hydrodynamic pressure on the fuselage bottom allows to understand the physics underling the interaction of the fuselage with the water.

Two formulations are used for the water domain in the ditching simulations: the first model is based on the ALE method while a hybrid Lagrangian-SPH discretisation is used in the second model. The differences in the results are related to the capability to simulate the complex hydrodynamic phenomena associated to the interaction of the fuselage with the water surface. The ALE model shows a good correlation with the experimental data but overestimates the suction forces acting on the fuselage. The magnitude of the longitudinal acceleration predicted by the ALE model is comparable to the vertical acceleration. This is an unusual loading condition for an aircraft and additional studies are required to investigate how it might affect the crashworthy design of the structure. The hybrid model cannot take into account for the suction effect and it results in the underestimation of the longitudinal forces acting on the fuselage.

Both models predict that the most severe loading condition, in terms of aircraft accelerations, does not occur

at the time of impact with the water surface. Therefore, the deceleration is mostly associated to the development of the hydrodynamic effects, i.e. suction, rather than to the momentum transmitted from the fuselage to the water during the impact.

Disclosure statement

No potential conflict of interest was reported by the authors.

References

[1] M. Anghileri, L.M. Castelletti, E. Francesconi, A. Milanese, and M. Pittofrati, *Rigid body water impact-experimental tests and numerical simulations using the SPH method*, Int. J. Impact. Eng. 38 (2011), pp. 141–151.

[2] M. Anghileri, L.M. Castelletti, E. Francesconi, A. Milanese, and M. Pittofrati, *Survey of numerical approaches to analyze the behavior of a composite skin panel during a water impact*, Int. J. Impact. Eng. 63 (2014), pp. 43–51.

[3] M. Anghileri and A. Spizzica, *Experimental validation of finite element models for water impacts*, Second International Krash Users' Seminar. Cranfield Impact Centre Ltd, England, 1995.

[4] D. Benson, *An efficient, accurate, simple ALE method for nonlinear finite element programs*, Comput. Methods Appl. Mech. Eng. 72 (1989), pp. 305–350.

[5] E.G. Candy, N.E. Kirk, and P.J. Murrell, *Airframe water impact analysis*, Int. J. Crashworthiness 5 (2000), pp. 51–62.

[6] H. Climent, L. Benitez, F. Rosich, F. Rueda, and N. Pentecote, *Aircraft ditching numerical simulation*, 25th International Congress of the Aeronautical Sciences, Hamburg, 2006.

[7] F.H. Collopy, *Determination of the water impact shock environment*, Shock Vib. Bull. 35 (1966), pp. 77–86.

[8] L.J. Fisher and E.L. Hoffman, *Ditching investigation of dynamic model and effects of design parameters on ditching characteristics*, NACA TN 3946, 1957.

[9] P.H.L. Groenenboom, J. Campbell, L.B. Montañés, and M. Siemann, *Innovative SPH method for aircraft ditching*, 11th World Congress on Computational Mechanics, Barcelona, 2014.

[10] P.H.L. Groenenboom and B.K. Cartwright, *Hydrodynamics and fluid-structure interaction by coupled SPH-FE method*, J. Hydraul. Res. 48 (2010), pp. 61–73.

[11] B. Guo, P. Liu, Q. Qu and J. Wang, *Effect of pitch angle on initial stage of a transport airplane ditching*, Chin. J. Aeronaut. 26 (2013), pp. 17–26.

[12] J.O. Hallquist, *LS-DYNA Theory Manual*, Livermore Software Technology Corporation, Livermore, CA, 2006.

[13] C. Hua and C. Fang, *Simulation of fluid-solid interaction on water ditching of an airplane by ALE method*, J. Hydrodyn. 23 (2011), pp. 637–642.

[14] K. Hughes and J. Campbell, *Helicopter crashworthiness: A chronological review of water impact related research from 1982 to 2006*, J. Am. Helicopter Soc. 53 (2008), pp. 429–442.

[15] K. Hughes, J. Campbell, and R. Vignjevic, *Application of the finite element method to predict the crashworthy response of a metallic helicopter under floor structure onto water*, Int. J. Impact Eng. 35 (2008), pp. 347–362.

[16] K. Hughes, R. Vignjevic, J. Campbell, T. De Vuyst, N. Djordjevic, and L. Papagiannis, *From aerospace to offshore: B ridging the numerical simulation gaps – S imulation advancements for fluid structure interaction problems*, Int. J. Impact Eng. 61 (2013), pp. 48–63.

[17] T.J.R. Hughes, W.K. Liu, and T.K. Zimmerman, *Lagrangian Eulerian finite elements formulation for viscous flows*, Comput. Methods Appl. Mech. Eng. 29 (1981), pp. 329–349.

[18] H. Lamb, *Hydrodynamics*, Cambridge University Press, Cambridge, UK, 1993.

[19] E.E. McBride and L.J. Fisher, *Experimental investigations of the effect of rear-fuselage shape on ditching behaviour*, NACA TN 2929, 1953.

[20] J.J. Monaghan, *Smoothed particle hydrodynamics*, Ann. Rev. Astr. Astroph. 30 (1992), pp. 543–574.

[21] National Transportation Safety Board, *Loss of thrust in both engines after encountering a flock of birds and subsequent ditching on the Hudson river US airways flight 1549*, NTSB/AAR-10/03, Accident Report NTSB/AAR-10/03, National Transportation Safety Board, May 4, Washington, DC, 2010.

[22] A.A. Patel and R.P. Greenwood Jr, *Transport water impact and ditching performance*, US Department of Transportation, Final report DOT/FAA/AR-95/54, 1996.

[23] N. Pentecôte and A. Vigliotti, *Crashworthiness of helicopters on water: T est and simulation of a full-scale WG30 impacting on water*, Int. J. Crashworthiness 8 (2003), pp. 559–572.

[24] C.M. Seddon and M. Moatamedi, *Review of water entry with applications to aerospace structures*, Int. J. Impact. Eng. 32 (2006), pp. 1045–1067.

[25] A.G. Smith, C.H.E. Warren, and D.F. Wright, *Investigations of the Behaviour of Aircraft When Making a Forced Landing on Water (Ditching)*, Aeronautical Research Council, London, UK, 1957.

[26] M. Souli and D.J. Benson (eds.), *Arbitrary Lagrangian-Eulerian and Fluid-Structure Interaction: Numerical Simulation*, ISTE, London, 2010.

[27] H. Streckwall, O. Lindenau, and L. Bensch, *Aircraft ditching: a free surface/free motion problem*, Arch. Civ. Mech. Eng. 7 (2007), pp. 177–190.

[28] W.C. Thompson, *Model ditching investigation of the Boeing 707 jet transport*, NACA Memorandum SL55K08, 1955.

[29] N. Toso, *Contribution to the modelling and simulation of aircraft structures impacting on water*, Ph.D. diss., Universität Stuttgart, 2009.

[30] R. Vignjevic and M. Meo, *Simulation of helicopter underfloor structure impact on water*, Int. J. Crashworthiness 6 (2001), pp. 425–443.

[31] R. Vignjevic and M. Meo, *A new concept for a helicopter sub-floor structure crashworthy in impacts on water and rigid surfaces*, Int. J. Crashworthiness 7 (2002), pp. 321–330.

[32] C. Violeau, *Fluid Mechanics and the SPH Method: Theory and Applications*, Oxford University Press, Oxford, 2012.

[33] T. Von Karman, *The impact of seaplane floats during landing*, Tech. Note NACA 321, Washington, DC, 1929.